

Electronic structure of the d^1 bent-metallocene Cp_2VCl_2 : A photoelectron and density functional study

Matthew A. Cranswick, Nadine E. Gruhn, John H. Enemark, Dennis L. Lichtenberger*

Department of Chemistry, The University of Arizona, Tucson, AZ 85721, USA

Received 19 October 2007; received in revised form 13 December 2007; accepted 17 December 2007

Available online 15 January 2008

In tribute to F. Albert Cotton for not just his teachings, but also for the excitement of discovery and new understanding in chemistry he brought to us and many others.

Abstract

The Cp_2VCl_2 molecule is a prototype for bent-metallocene complexes with a single electron in the metal d shell, but experimental measure of the binding energy of the d electron by photoelectron spectroscopy eluded early attempts due to apparent decomposition in the spectrometer to Cp_2VCl . With improved instrumentation, the amount of decomposition is reduced and subtraction of ionization intensity due to Cp_2VCl from the Cp_2VCl_2/Cp_2VCl mixed spectrum yields the Cp_2VCl_2 spectrum exclusively. The measured ionization energies provide well-defined benchmarks for electronic structure calculations. Density functional calculations support the spectral interpretations and agree well with the ionization energy of the d^1 electron and the energies of the higher positive ion states of Cp_2VCl_2 . The calculations also account well for the trends to the other Group V bent-metallocene dichlorides Cp_2NbCl_2 and Cp_2TaCl_2 . The first ionization energy of Cp_2VCl_2 is considerably greater than the first ionization energies of the second- and third-row transition metal analogues.

© 2008 Elsevier B.V. All rights reserved.

Keywords: Vanadium; Bent-metallocenes; Photoelectron spectroscopy; Density functional theory

1. Introduction

The chemistry of bent-metallocene complexes has been a major factor in the development of organometallic chemistry over the last 50 years [1–5], finding applications in diverse fields ranging from polymer catalysis [4,6,7] to cancer research [8–11]. The electron configuration and subsequent reactivity of the metal center can be fine-tuned with the choice of metal, cyclopentadienyl substituents, and additional coordinating ligands. Elucidating the electronic structure of bent-metallocenes is important in understanding the chemical behavior and physical properties of these complexes. Photoelectron spectroscopy provides an experimental measure of the orbital energetics and interac-

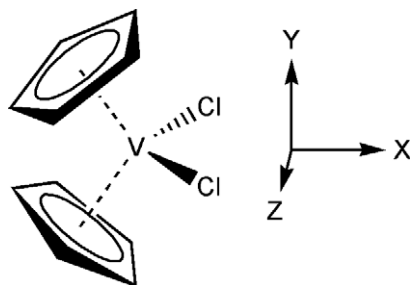
tions and at this point there is a general understanding of the photoelectron spectra of simple metallocenes [7,12,13]. One remaining point of contention has been the reported photoelectron spectrum of Cp_2VCl_2 , which has been an outlier from all other reported metallocene photoelectron results. This has been unfortunate because Cp_2VCl_2 is a prototype for d^1 bent-metallocene complexes, having a first-row transition metal, relatively simple ligands, and sufficient symmetry to be a foundational model for other studies.

The electronic structure of Cp_2VCl_2 has previously been investigated by electron paramagnetic resonance (EPR) [14–17] and photoelectron spectroscopy (PES) [15]. EPR experiments concluded that the unpaired metal electron resides in an orbital composed primarily of d_{z^2} character in the VCl_2 plane as depicted in the coordinates below, with some admixture of $d_{x^2-y^2}$ character. Photoelectron studies of Cp_2VCl_2 and $(C_5H_4Me)_2VCl_2$ [15,18] revealed spectra

* Corresponding author.

E-mail address: dlichten@email.arizona.edu (D.L. Lichtenberger).

that were similar in structure to those of their Ti analogues, but with two low energy ionization features. Only one low energy ionization was expected for the single d electron in the vanadium complexes. The possibility of decomposition was investigated and considered less likely for the $(C_5H_4Me)_2VCl_2$ molecule. The lowest energy feature of the spectrum obtained from the $(C_5H_4Me)_2VCl_2$ sample at 6.60 eV was tentatively assigned to the metal d^1 ionization. The second feature at 7.20 eV was hypothesized to be a triplet component of the unpaired d^1 electron exchange splitting with the Cl $p\pi$ orbitals. The singlet component of this ionization could then contribute to broadening of the next band, rather than appear as a separate band. This assignment was called into doubt when it was found that the related Nb and Ta complexes had only one low energy ionization consistent with their d^1 configurations [12,18]. Subsequent photoelectron studies of Cp_2VCl [19], which has a high-spin d^2 configuration, showed bands at 6.80 and 7.40 eV. The spectrum of this monochloride complex appeared similar to the reported spectrum of the dichloride complex, suggesting that Cp_2VCl_2 may be decomposing to Cp_2VCl during the photoelectron experiment. Cp_2VCl_2 is known to undergo thermal- [15] and photoelectrochemical decomposition [20] to Cp_2VCl during other experimental conditions.



Recently, we investigated the electronic structure of bent vanadocene dithiolates as minimum molecular models of the d^1 electron configuration of sulfite oxidizing enzymes using photoelectron spectroscopy and density functional theory [21]. This study prompted us to reinvestigate the electronic structure of the simplest d^1 bent-metallocene, Cp_2VCl_2 , in more detail to aid in the interpretation of the vanadocene dithiolate spectra. Improved gas-phase photoelectron spectroscopy techniques, comparison to the photoelectron spectra of Cp_2VCl and other Group V metallocene dichlorides, along with DFT calculations, have allowed us to isolate and reassign the photoelectron spectrum of Cp_2VCl_2 for determination of the ionization energy of the d^1 electron.

2. Results and discussion

2.1. Photoelectron spectroscopy

The low energy valence regions of the gas-phase photoelectron (PES) spectra collected from samples of Cp_2VCl

and Cp_2VCl_2 are presented in Fig. 1. The spectra obtained using typical data collection techniques are in agreement with spectra previously reported in the literature [15,19]. There is a large similarity between the two spectra obtained from the Cp_2VCl and Cp_2VCl_2 samples, Fig. 1A and B respectively, which would not be expected given the anticipated relative ionizations from the high-spin d^2 metal center of Cp_2VCl versus the d^1 metal center of Cp_2VCl_2 . When a spectrum of the Cp_2VCl_2 sample is recorded using sample entry procedures designed to minimize decomposition (see Section 4), the overall shape of the spectrum changes dramatically (Fig. 1C). Most importantly, the relative intensity of the ionization at 6.8 eV decreases substantially relative to the ionization at 7.4 eV. In addition, ionization intensity in the region labeled L3 in the spectrum of Cp_2VCl decreases while the ionization intensity in the region of L2 increases. The similarities in the spectra 1A and 1B and the differences between these and spectrum 1C are strong evidence that Cp_2VCl_2 is decomposing to Cp_2VCl in the spectrometer. The decomposition has been minimized, but not completely eliminated, as evidenced by the small amount of ionization intensity remaining at 6.8 eV in Fig. 1C. The remaining ionization intensity in spectrum 1C from Cp_2VCl cannot be due to residual Cp_2VCl in the Cp_2VCl_2 sample because the sublimation temperature of Cp_2VCl is approximately 100 °C lower than that of Cp_2VCl_2 (see Section 4) and would be observed first as the temperature of the sample cell rises. Also, this contamination cannot be due to photoelectrochemical dehalogenation [20] of the solid sample since the sample is in the

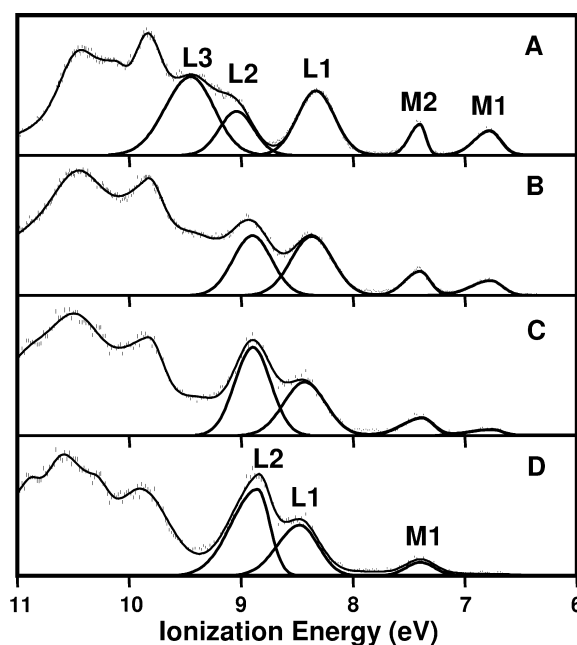


Fig. 1. Low energy He I spectra showing the extraction of the Cp_2VCl_2 spectrum from the data: (A) spectrum of Cp_2VCl , (B) spectrum of Cp_2VCl_2 sample loaded directly into ionization chamber, (C) spectrum of Cp_2VCl_2 sample effused directly into photon beam from a quartz crucible, (D) subtraction of A from C to give difference Cp_2VCl_2 spectrum.

direct path of the ionization source during the experiment and Cp_2VCl is not seen at lower temperatures, nor were ionizations found corresponding to the photochemical product Cl_2 . Therefore, it is hypothesized that use of the quartz crucible and the short path to the photon beam reduces surface interactions of Cp_2VCl_2 with the aluminum sample cell, which may lead to reduction and dehalogenation of Cp_2VCl_2 . It was noted that, during the experiment, a sharp doublet-ionization occurs at 12.75 and 12.82 eV, coincident with the first ionizations of HCl. The ionization intensity due to Cp_2VCl in Fig. 1C is removed by subtracting the Fig. 1A spectrum, appropriately scaled to the ionization of Cp_2VCl at 6.8 eV in Fig. 1C, to yield the spectrum shown in Fig. 1D. The ionizations shown in Fig. 1D are taken to be those of Cp_2VCl_2 . The subtraction of the Cp_2VCl spectrum leads to a shape (width and symmetry) for the first ionization of Cp_2VCl_2 at 7.40 eV that is indicative of a single ionization [22].

Fig. 2 shows that the resultant Cp_2VCl_2 spectrum bears strong similarities to the He I photoelectron spectra of Cp_2NbCl_2 and Cp_2TaCl_2 [12]. The ionization region of ~8–9.8 eV is particularly diagnostic, because this region contains ionizations that are symmetry combinations of the $p\pi$ orbitals of the two Cl atoms with the metal. The similar ionization pattern in this region indicates similar MCl_2 structure for the three molecules. The main difference between the spectra of Cp_2MCl_2 ($M = \text{V}, \text{Nb}, \text{Ta}$) (Fig. 2) is the energy of the metal d^1 ionization, which can be ascribed to reduction of the effective nuclear charge on going from 3d to 4d to 5d, reflecting the shielding of the unpaired electron by the different atoms.

Table 1 shows the analytical representation of the ionizations for Cp_2VCl_2 and Cp_2VCl . This table includes the

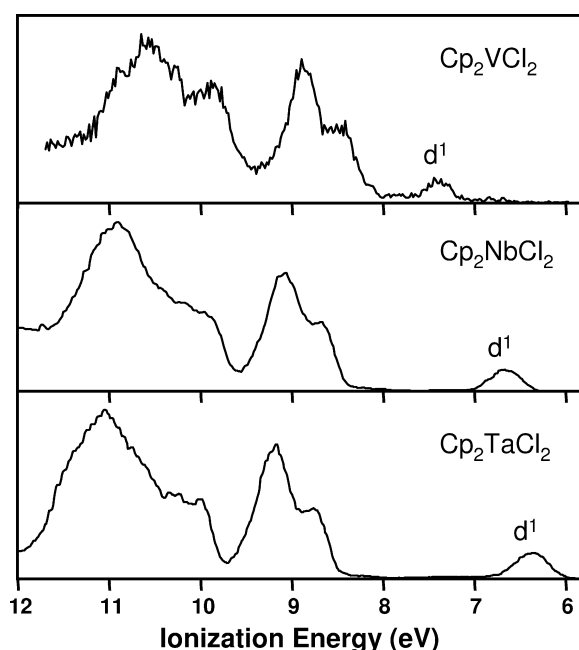


Fig. 2. He I photoelectron spectra of Cp_2VCl_2 , Cp_2NbCl_2 and Cp_2TaCl_2 .

change in band area with change in ionization source from He I to He II for Cp_2VCl . Green et al. have previously assigned the photoelectron spectrum of Cp_2VCl based on a He I/He II comparison and their assignments are reflected in Table 2 [19]. The predominant Cl $p\pi$ character mentioned above in ionizations labeled L1 and L2 is evidenced by their decrease in ionization intensity relative to the metal-based ionizations from He I to He II excitation.

2.2. Computational results

A central question concerns the ability of electronic structure calculations to account for the geometric structures and the electron energies and distributions of open-shell bent-metallocene complexes of the early transition metals. The calculated structures of Cp_2VCl_2 and Cp_2VCl are compared with the reported structures determined from X-ray crystallography in Table 3 [23,24]. The structures agree reasonably well with the largest deviation being the V–Cl bond distance in Cp_2VCl_2 which is underestimated by about 0.04 Å. The ground states of these molecules are calculated as an unrestricted doublet and triplet, respectively for Cp_2VCl_2 and Cp_2VCl . Spin contamination is minimal, giving a value of 0.78 compared to the ideal value for $s(s+1)$ of 0.75 for Cp_2VCl_2 and 2.05 compared to the ideal value of 2.00 for Cp_2VCl .

DFT calculations were also used to model the electron density in the highest occupied molecular orbital (HOMO) for comparison with EPR studies. The trend of the Cl–M–Cl angle to decrease from Ti to V to Mo for the d^0 to d^1 to d^2 configurations and the single crystal EPR studies on the d^1 complexes led to the conclusion that the HOMO of the V and Mo compounds is primarily along an axis normal to the plane bisecting the Cl–M–Cl angle. Lowering the symmetry of Cp_2VCl_2 from C_{2v} to C_s allows this axis to be labeled z , as illustrated in Section 1. If the ligand contributions

Table 1
Analytical representation of the ionization features of Cp_2VCl_2 and Cp_2VCl obtained with He I and He II photon sources

Band	IE ^a (eV)	Band width ^b		Relative area ^c	
		High (eV)	Low (eV)	He I	He II
<i>Cp₂VCl₂</i>					
M1	7.40	0.30	0.30	1	
L1	8.47	0.47	0.38	5.42	
L2	8.85	0.55	0.26	8.80	
<i>Cp₂VCl</i>					
M1	6.78	0.33	0.23	1	1
M2	7.40	0.22	0.12	0.78	0.97
L1	8.33	0.39	0.39	3.67	1.41
L2	9.04	0.36	0.36	2.32	1.41
L3	9.45	0.54	0.49	5.92	4.22

^a Vertical ionization energy defined as the position of the asymmetric Gaussian peak modeling the band.

^b Widths of the asymmetric Gaussian peak modeling the high and low ionization energy sides of the band.

^c Band areas are relative to an area of 1 for M1.

Table 2
Experimental and calculated ionization energies (eV) for Cp₂VCl₂ and Cp₂VCl

Band	IE ^a	Assignment	Kohn–Sham		ΔSCF ^c	
			Orbital energy ^b			
<i>Cp₂VCl₂</i>						
M1	7.40	V d _{z²}	α-Spin −4.83 (7.40)	β-Spin	Singlet 7.27	Triplet
L1	8.47	Cl pπ	−5.81 (8.38)	−5.78 (8.35)	8.20	8.15
L2	8.85	Cl pπ	−5.96 (8.53)	−5.88 (8.45)	8.49	8.44
<i>Cp₂VCl</i>						
M1	6.78	V d _{xz}	α-Spin −4.24 (6.78)	β-Spin	Doublet 6.85	Quartet
M2	7.40	V d _{z²}	−4.87 (7.41)		7.56	
L1	8.33	Cl pπ	−5.64 (8.18)	−5.59 (8.13)	8.33	8.18
L2	9.04	Cl pπ	−6.65 (9.19)	−6.34 (8.88)	9.27	8.91
L3	9.45	Cp pπ + Cl pπ	−7.17 (9.71)	−6.93 (9.47)	9.50	9.24

^a Experimental vertical ionization energy in eV.

^b The values in parentheses are the orbital energies shifted by an amount such that the first orbital energy matches the first ionization energy.

^c The difference in total energy between the molecular ground state and the molecule with an electron removed from the specified orbital.

Table 3
Comparison of the calculated geometries with the crystallographic molecular structures for Cp₂VCl₂ and Cp₂VCl^a

	Calculated	Experimental
<i>Cp₂VCl₂</i> ^b		
Cp _{C–C}	1.403–1.428 (1.415) ^c	1.371–1.465 (1.418) 1.394–1.457 (1.424)
M–Cp _{centroid}	1.952, 1.948	1.983, 1.967 1.971, 1.986
M–C	2.231–2.306 (2.269)	2.281–2.368 (2.314) 2.284–2.342 (2.315)
M–Cl	2.371	2.409, 2.418 2.410, 2.411
Cl–M–Cl	88.74 ^c	86.6 ^c 87.1 ^c
<i>Cp₂VCl</i> ^d		
Cp _{C–C}	1.406–1.420 (1.413)	1.379–1.408 (1.394)
M–Cp _{centroid}	1.901, 1.901	1.946, 1.944
M–C	2.221–2.277 (2.250)	2.261–2.296 (2.278)
M–Cl	2.367	2.390

^a All distances are given in Å.

^b Crystallographic data taken from Tzavellas et al. [23].

^c Average distance.

^d Crystallographic data taken from Fieselmann et al. [24].

are neglected then $|\Psi_{\text{HOMO}}\rangle = a|d_{z^2}\rangle + b|d_{x^2-y^2}\rangle$. Previous Fenske–Hall [25] molecular orbital percent characters in the singly-occupied orbital were calculated to be 20.5/1 for d_{z²}/d_{x²–y²} in Cp₂VCl₂, which agrees well with the ratio obtained from the EPR data for (C₆H₅Me)₂VCl₂ of 20.0/1 [15]. Using current DFT methods, the singly-occupied orbital of Cp₂VCl₂ is calculated to be 60.8% d_{z²} and 3.44% d_{x²–y²} giving a ratio of 17.7:1. This ratio is similar to the orbital percent characters calculated using the Fenske–Hall method and the observed orbital parameters calculated from the EPR experiment.

The energies of the ionizations observed for Cp₂VCl₂ and Cp₂VCl by photoelectron spectroscopy are compared with those calculated by the ΔSCF method and with the

Kohn–Sham orbital energies (Table 2). The calculated Kohn–Sham orbital energies from the DFT calculations are related to the photoelectron ionization energies by applying a corollary to Koopmans' theorem from Hartree–Fock calculations [26]. Koopmans' theorem has intrinsic uncertainty including electron relaxation, electron correlation, relativistic effects, vibronic coupling, and differences in spin states [27–34], which can lead to poor correlation between the calculated orbital energies and the ionization potentials. A central principle of the Kohn–Sham orbital model is that the negative of the Kohn–Sham orbital energy for the HOMO, calculated with the correct functional and basis, will exactly match the first ionization energy of the molecule, but in current practice these energies differ substantially. Nonetheless, the relative energies of the Kohn–Sham orbitals can be useful in interpreting the pattern of ionizations. ΔSCF calculations were performed to account for the deficiencies in the frozen orbital approximation and to get information on the coupling of electron spins.

The ground state of neutral Cp₂VCl₂ is $s = \frac{1}{2}$ (V⁴⁺, d¹, ²A') while the ground state of Cp₂VCl is $s = 1$ (high-spin V³⁺, d², ³A''). Fig. 3 shows the contour plots for the spin α and β orbitals of Cp₂VCl₂ that correspond to the ionizations evaluated in this study by PES. For Cp₂VCl₂, ionization from the singly-occupied HOMO will lead to a singlet state, while ionization from the doubly-occupied ligand-based orbitals leads to both singlet and triplet state configurations with coupling to the d¹ electron. For Cp₂VCl, ionization from the singly-occupied HOMO and HOMO–1 lead to doublet states, and ionization from the doubly-occupied ligand-based orbitals will lead to either doublet or quartet state configurations. Table 2 shows the calculated values for the singlet/triplet states of Cp₂VCl₂ and doublet/quartet states of Cp₂VCl using the ΔSCF method. For Cp₂VCl₂, the calculated singlet/triplet state separation is only 0.05 eV for both ionizations L1

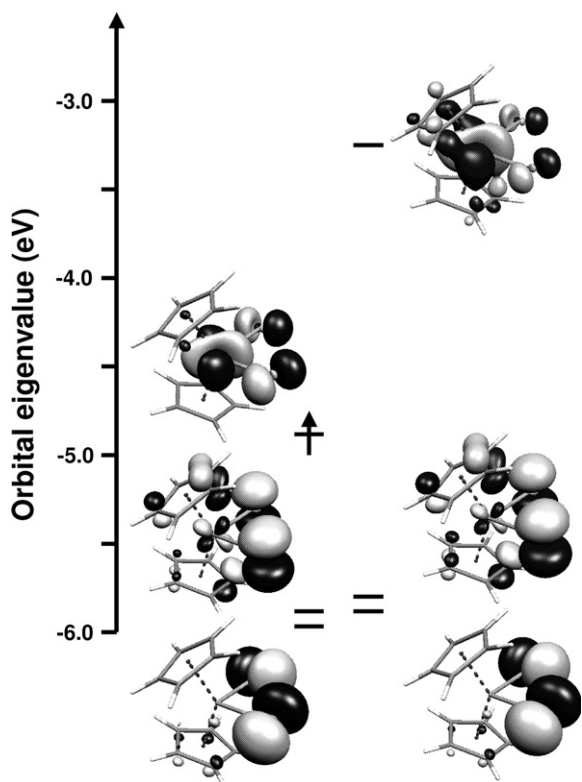


Fig. 3. Spin correlation diagram for Cp_2VCl_2 showing α - and β -spin molecular orbital character and electron occupations.

and L2, and therefore ionizations to these individual states are not likely to be resolved in the photoelectron spectrum. For Cp_2VCl the calculated doublet/quartet state separation for band L1 is 0.15 eV, still less than the 0.4 eV width of the unresolved vibrational broadening of the band. For bands L2 and L3, the calculated doublet/quartet state separations are 0.36 and 0.26 eV, respectively; however, these bands are now in a region of overlapping ionizations that preclude observation of individual states.

ΔSCF calculations for Cp_2VCl_2 predict the singly-occupied HOMO ionization to be at 7.27 eV, consistent with the first ionization of Cp_2VCl_2 at 7.40 eV (Table 2). The calculated ΔSCF ionizations for L1 and L2 are also similar with the HOMO–1 and HOMO–2 ionizations, and follow the ionization trend. The shifted Kohn–Sham orbital energies for L1 and L2 are also similar to the observed ionization energies. ΔSCF calculations were also performed on Cp_2VCl to confirm that removing an electron from the triplet ground state d orbital configuration will give a metal ionization that coincides with removing an electron from the HOMO of Cp_2VCl_2 . Table 2 shows that removing an electron from the HOMO–1 of Cp_2VCl gives a ΔSCF calculated ionization energy of 7.56 and a shifted Kohn–Sham orbital energy of 7.41, coincident with the HOMO ionization of Cp_2VCl_2 . Both the ΔSCF method and shifted Kohn–Sham orbital energies follow similar trends to the observed ionization energies for Cp_2VCl . These calculations support that subtraction of the Cp_2VCl spectral contribution from the mixed $\text{Cp}_2\text{VCl}_2/\text{Cp}_2\text{VCl}$ spectrum is

effective for revealing the Cp_2VCl_2 spectrum. The first ionization of Cp_2NbCl_2 and Cp_2TaCl_2 was also calculated by the ΔSCF method to be 6.65 and 6.37 eV, almost exactly coincident to the observed ionization energies of 6.69 and 6.39 eV [12].

3. Conclusions

We have revisited the gas-phase photoelectron spectrum of Cp_2VCl_2 and used improved collection techniques to reduce the Cp_2VCl decomposition product from the Cp_2VCl_2 He I spectrum. Subtraction of ionization intensity due to the Cp_2VCl decomposition product leads to a Cp_2VCl_2 spectrum that is similar in appearance to other Group V bent-metallocene dichlorides. Density functional theory calculations support the assignments made for the Cp_2VCl_2 spectrum and comparison to the calculated ionization energies for Cp_2VCl also confirm that the d^1 ionization of Cp_2VCl_2 coincides with one of the metal ionizations of Cp_2VCl , further supporting the superposition of the Cp_2VCl and Cp_2VCl_2 spectra. The open-shell calculations on these Group V bent-metallocenes show good reliability in calculating the geometric structures and electron distributions and give good account of the ionization energies using either the shifted Kohn–Sham orbital energies or the ΔSCF method.

4. Experimental methods

4.1. Photoelectron spectroscopy

Samples of Cp_2VCl (97%) and Cp_2VCl_2 (95%) were purchased through Aldrich and used as received. Photoelectron spectra were recorded using an in-house instrument built around a 36 cm hemispherical analyzer (McPherson), custom-designed sample cells and detection and control electronics. The electron detection and instrument operation are interfaced to a National Instruments PCIe-6259 multi-function data acquisition card and custom software. Argon was used as an internal calibrant during data collection and the instrument resolution (measured using FWHM of the argon $^2\text{P}_{3/2}$ peak) was 0.020–0.030 eV. The sublimation temperatures (at 10^{-5} Torr, monitored using a “K” type thermocouple passed through a vacuum feed-through and attached directly to the sample cell) were 195–205° for Cp_2VCl_2 and 90–120° for Cp_2VCl . For Cp_2VCl_2 , a crushed crystalline sample was placed in a quarter-inch diameter quartz crucible that was inserted into the ionization chamber of the sample cell directly below the photon beam [35,36].

In the photoelectron spectra, the vertical length of each data mark represents the experimental variance of that point. The valence ionization bands are represented analytically with the best fit of asymmetric Gaussian peaks [22]. The number of peaks used in a fit was based solely on the features of a given band profile. The peak positions are reproducible to about ± 0.02 eV ($\approx 3\sigma$). The parameters

describing an individual Gaussian peak are less certain when two or more peaks are close in energy and overlap.

4.2. Theoretical methods

The Amsterdam density functional theory suite (ADF 2006.01, using the standard parameters except for the options given in parentheses) was used to study the electronic structure of Cp_2MCl_2 ($\text{M} = \text{V}, \text{Nb},$ and Ta) and Cp_2VCl . The optimized geometries of Cp_2MCl_2 and Cp_2VCl were constructed in C_s symmetry using the crystal structures as a starting point. In C_s symmetry, the Cp rings were staggered and the mirror plane is coincident with the xy plane, which bisects and each Cp ring and the Cl–V–Cl angle of Cp_2VCl_2 or lies along the V–Cl bond of Cp_2VCl . Calculations on the ground state and excited state ions were conducted in the spin unrestricted mode (unrestricted) since Cp_2VCl and Cp_2MCl_2 contain two and one unpaired electrons, respectively. A generalized gradient approximation, with the correlation of Perdew et al. [37] and exchange correction of Handy and Cohen [38] (GGA OPBE), was used. This functional has been found by us [21,39–41] and others [42–45] to give reasonable geometry parameters, spin states, and ionization and oxidation potentials. The calculations employed Slater-type orbitals for basis sets with double-zeta valence plus polarization functions for main group elements and triple-zeta valence plus polarization functions for the metal (DZP for C, H, and Cl, and TZP for V, Nb and Ta). Geometry optimizations were also carried out using integration to six significant figures (integraton = 6.0), using the zeroth-order relativistic approximation (ZORA), using tighter convergence criteria for the energy, bond distances and angles ($E = 0.0005$, grad = 0.001, rad = 0.0005), using the smoothing of gradients (aggressive) option, and the convergence of the self-consistent field was tightened (converge $1e-6$ $1e-6$).

ASCF calculations of the ionized states were performed at the fixed geometry of the neutral molecule, with one electron removed from the relevant orbital. For the ligand-based ionizations both singlet and triplet ionized states for Cp_2VCl_2 and doublet and quartet ionized states for Cp_2VCl were calculated. The ΔSCF estimate of the ionization energy is the difference between the calculated total energy of the ionized state and that of neutral ground state molecule. As is customary for larger polyatomic molecules with low frequency vibrational modes, a semi-classical treatment of the ionization intensity is assumed that neglects zero-point vibrational energies (ZPEs). This semi-classical interpretation is reasonable since the low-frequency vibrational modes give an essentially continuum, vibrationally unresolved band in the photoelectron spectrum.

Acknowledgements

We gratefully acknowledge support of this research by the National Institutes of Health (Grant GM-37773 to

J.H.E.), the National Science Foundation (Grant CHE 0416004 to D.L.L.), and a Galileo Circle Scholarship (sponsored by Proctor & Gamble Co. to M.A.C.).

References

- [1] J.W. Lauher, R. Hoffmann, *J. Am. Chem. Soc.* 98 (1976) 1729–1742.
- [2] F.A. Cotton, G. Wilkinson, C.A. Murillo, M. Bochmann, *Advanced inorganic chemistry*, 6th ed., John Wiley and Sons, New York, 1999, pp. 689–691.
- [3] M.M. Harding, G. Mokdsi, *Curr. Med. Chem.* 7 (2000) 1289–1303.
- [4] J.A. Gladysz, *Chem. Rev.* 100 (2000) 1167–1168.
- [5] Y. Yamaguchi, W. Ding, C.T. Sanderson, M.L. Borden, M.J. Morgan, C. Kutal, *Coord. Chem. Rev.* 251 (2007) 515–524.
- [6] C.E. Carraher, *J. Inorg. Organomet. Polym. Mater.* 15 (2005) 121–145.
- [7] J.C. Green, *Chem. Soc. Rev.* 27 (1998) 263–272.
- [8] J.H. Toney, C.P. Brock, T.J. Marks, *J. Am. Chem. Soc.* 108 (1986) 7263–7274, and references therein.
- [9] I. Pavlik, J. Vinklarek, *Eur. J. Solid State Inorg. Chem.* 28 (1991) 815–827.
- [10] J. Vinklarek, J. Honzicek, J. Holubova, *Inorg. Chim. Acta* 357 (2004) 3765–3769.
- [11] J.B. Waern, H.H. Harris, B. Lai, Z.H. Cai, M.M. Harding, C.T. Dillon, *J. Biol. Inorg. Chem.* 10 (2005) 443–452.
- [12] G.P. Darsey, Ph.D. dissertation, The University of Arizona, 1988, p. 165.
- [13] S. Barlow, H.E. Bunting, C. Ringham, J.C. Green, G.U. Bublitz, S.G. Boxer, et al., *J. Am. Chem. Soc.* 121 (1999) 3715–3723.
- [14] J.L. Petersen, L.F. Dahl, *J. Am. Chem. Soc.* 96 (1974) 2248–2250.
- [15] J.L. Petersen, D.L. Lichtenberger, R.F. Fenske, L.F. Dahl, *J. Am. Chem. Soc.* 97 (1975) 6433–6441.
- [16] J.L. Petersen, L.F. Dahl, *J. Am. Chem. Soc.* 97 (1975) 6416–6422.
- [17] J.L. Petersen, L.F. Dahl, *J. Am. Chem. Soc.* 97 (1975) 6422–6433.
- [18] C. Cauletti, J.P. Clark, J.C. Green, S.E. Jackson, I.L. Fragala, E. Ciliberto, et al., *J. Electron Spectrosc. Relat. Phenom.* 18 (1980) 61–73.
- [19] J.C. Green, M.P. Payne, J. Teuben, *Organometallics* 2 (1983) 203–210.
- [20] R.G. Compton, J. Booth, J.C. Eklund, *J. Chem. Soc., Dalton Trans. Inorg. Chem. (1972–1999)* (1994) 1711–1715.
- [21] M.A. Cranswick, A. Dawson, J.J.A. Cooney, N.E. Gruhn, D.L. Lichtenberger, J.H. Enemark, *Inorg. Chem.* 46 (2007) 10639–10646.
- [22] D.L. Lichtenberger, A.S. Copenhaver, *J. Electron Spectrosc. Relat. Phenom.* 50 (1990) 335–352.
- [23] N. Tzavellas, N. Klouras, C.P. Raptopoulou, *Z. Anorg. Allg. Chem.* 622 (1996) 898–902.
- [24] B.F. Fieselman, G.D. Stucky, *J. Organometal. Chem.* 134 (1977) 43.
- [25] M.B. Hall, R.F. Fenske, *Inorg. Chem.* 11 (1972) 768–775.
- [26] T. Koopmans, *Physica* 1 (1933) 104–113.
- [27] W.G. Laidlaw, F.W. Birss, *Theoret. Chim. Acta* 2 (1964) 181–185.
- [28] M.D. Newton, *J. Chem. Phys.* 48 (1968) 2825.
- [29] J.L. Dodds, R. McWeeny, *Chem. Phys. Lett.* 13 (1972) 9.
- [30] L.S. Cederbaum, G. Hohlneic, W. Niessen, *Chem. Phys. Lett.* 18 (1973) 503–508.
- [31] L.S. Cederbaum, *Chem. Phys. Lett.* 25 (1974) 562–563.
- [32] R. Dekock, *Chem. Phys. Lett.* 27 (1974) 297–299.
- [33] M.C. Bohm, *Theoret. Chim. Acta* 61 (1982) 539–558.
- [34] R. Stowasser, R. Hoffmann, *J. Am. Chem. Soc.* 121 (1999) 3414–3420.
- [35] J.L. Hubbard, Ph.D. Dissertation, The University of Arizona, 1982.
- [36] M.E. Jatko, Ph.D. Dissertation, The University of Arizona, 1990.
- [37] J.P. Perdew, K. Burke, Y. Wang, *Phys. Rev. B* 54 (1996) 16533–16539.
- [38] N.C. Handy, A.J. Cohen, *Mol. Phys.* 99 (2001) 403–412.
- [39] J.J.A. Cooney, M.A. Cranswick, N.E. Gruhn, H.K. Joshi, J.H. Enemark, *Inorg. Chem.* 43 (2004) 8110–8118.

- [40] G.A.N. Felton, A.K. Vannucci, J.-Z. Chen, L.T. Lockett, N. Okumura, B.J. Petro, et al., *J. Am. Chem. Soc.* 129 (2007) 12521–12530.
- [41] M.A. Cranswick, N.E. Gruhn, O. Oorhles-Steele, K.R. Ruddick, N. Burzlaff, W.A. Schenk, et al., *Inorg. Chim. Acta* (2008), doi:10.1016/j.ica.2007.08.021.
- [42] M. Swart, J.G. Snijders, *Theor. Chem. Acc.* 110 (2003) 34–41.
- [43] M. Swart, A.W. Ehlers, K. Lammertsma, *Mol. Phys.* 102 (2004) 2467–2474.
- [44] Y. Zhang, A.N. Wu, X. Xu, Y.J. Yan, *Chem. Phys. Lett.* 421 (2006) 383–388.
- [45] S.F. Sousa, P.A. Fernandes, M.J. Ramos, *J. Phys. Chem. A* 111 (2007) 10439–10452.